

NUMERICAL IMPLEMENTATION OF THE BLOCH EQUATIONS TO SIMULATE MAGNETIZATION DYNAMICS AND IMAGING

H. BENOIT-CATTIN¹, G. COLLEWET²

¹ CREATIS, UMR CNRS #5515, U 630 Inserm, Université Claude Bernard Lyon 1, INSA Lyon, Bât. B. Pascal, 69621 Villeurbanne, France.

² CEMAGREF / Food Processes Engineering Research Unit, 17 av de Cucillé, 35044 Rennes, France.

Abstract

The Bloch equations, that describe the behavior of a magnetization vector in the presence of magnetic fields, play a great role in MRI simulation. Indeed, these equations have been used in 1984 to design the first MRI simulator and are still the core of the most advanced MRI simulators. In the first part of this tutorial, we present the Bloch equations and we detail their discrete time solutions that are implemented in MRI simulators. In a second part, as an example of advanced MRI simulation, we focus on the SIMRI simulator [1]. We give an overview of its organization, of its object modeling, of its field modeling and we comment many examples of simulations.

1. INTRODUCTION

The simulation of Magnetic Resonance Imaging (MRI) is an important counterpart to MRI acquisitions. Simulation is naturally suited to acquire understanding of the complex MR phenomena [2]. It is used as an educational tool in medical and technical environments [3, 4]. MRI simulation also permits the investigation of artifact causes and effects [1, 5-7]. Likewise, MRI simulation may help in the development and optimization of MR sequences [5].

With the increased interest in computer-aided MRI image analysis methods (segmentation, data fusion, quantization ...), there is a greater need for objective methods of algorithm evaluation. Validation of in vivo MRI studies is complicated by a lack of reference data (gold standard) and the difficulty of constructing anatomical realistic physical phantoms. In this context, an MRI simulator provides an interesting assessment tool [8] since it generates 3D realistic images from medical virtual objects perfectly known.

The Bloch equations, that describe the behavior of a magnetization vector in the presence of magnetic fields, play a great role in MRI simulation. Indeed, these equations have been used in 1984 to design the first MRI simulator [9] and are still the core of the most advanced MRI simulators.

The first MRI simulator was proposed in 1984 by Bittoun et al. [9]. Based on the discrete time solution of the Bloch equations (See section 2.2), it enables 1D MRI simulation from a 1D discrete object that is defined at each voxel by the proton density ρ and the two time constants T_1 and T_2 . The global MRI signal is obtained by discrete summation of all object magnetization vectors. In 1995, using a similar strategy, Olsson et al. [6] performed 2D MRI simulations. Few years later, the MRI simulation capability was extended by a distributed implementation proposed by Brenner et al. [5]. In 1999, Kwan et al. [10] achieved simulation of 3D brain MRI images. Their simulation is still based on Bloch equations, but in order to face the simulation time problem, the object description is done through tissue template. Each template gives a tissue description through a high number of isochromats with their associated (ρ, T_1, T_2) values and resonance frequency. The images are then formed by weighing the tissue distribution for each voxel with each tissue signal computed using the Bloch equations.

This approach is very interesting regarding the simulation of intra-voxel heterogeneities. But it does not simulate the whole image formation process and as a consequence, it is not possible to simulate the artifacts associated to the coding gradients. Recently, using a multi component object model, Yoder et al. [7] and Benoit-Cattin et al. [1] proposed simulators that simulate properly the chemical shift artifact and that take into account the field default associated to the object to simulate MRI images with susceptibility artifact.

In the first part of this tutorial, we present the Bloch equations and we detail their discrete time solutions that are the core of the current MRI simulators. In a second part, as an example of advanced MRI simulation, we focus on the *SIMRI* simulator [1]. We give an overview of its organization, of its object modeling and of its field modeling, and we comment many examples of simulations.

2. BLOCH EQUATIONS

2.1 General expression

The Bloch equations [11], used for MRI simulations, give the time evolution of a spin magnetization vector $\vec{M} = (M_x, M_y, M_z)^T$ at a given position (x, y, z) by:

$$\frac{d\vec{M}}{dt} = \gamma \cdot (\vec{M} \times \vec{B}) - \begin{pmatrix} M_x / T_2 \\ M_y / T_2 \\ (M_z - M_0) / T_1 \end{pmatrix} \quad (1)$$

where M_0 is the spin magnetization equilibrium value which depends of the proton density ρ , (T_1, T_2) are the relaxation constants and γ is the gyromagnetic constant of the considered isochromat (42.58 MHz/T for the water proton). The local magnetic field B is modeled as follows:

$$B(\vec{r}, t) = B_0 \vec{z} + \Delta B(\vec{r}) \cdot \vec{z} + (\vec{G}(t) \cdot \vec{r}) \cdot \vec{z} + \vec{B}_1(t) \quad (2)$$

where B_0 is the main static magnetic field, $\Delta B(\vec{r})$ is the local field inhomogeneities, $\vec{G}(t)$ is the applied field gradient, $\vec{B}_1(t)$ is the RF pulse and $\vec{r} = (x, y, z)^T$ is the spatial coordinate.

2.2 Discrete time solution

The MRI simulation kernels implement a discrete time solution of the Bloch equations [9] by the means of rotation matrices and exponential scaling depending on the magnetic events of the MRI sequence. The magnetization vector evolution is iteratively computed according to the following equation:

$$\vec{M}(\vec{r}, t + \Delta t) = Rot_z(\theta_g) \cdot Rot_z(\theta_i) \cdot R_{relax} \cdot R_{RF} \cdot \vec{M}(\vec{r}, t) \quad (3)$$

where $Rot_z(\theta)$ is a rotation matrix about the z axis associated to the angle θ by:

$$Rot_z(\theta) = \begin{pmatrix} \cos\theta & \sin\theta & 0 \\ -\sin\theta & \cos\theta & 0 \\ 0 & 0 & 1 \end{pmatrix} \quad (4)$$

where θ_g is linked to the applied gradient $\vec{G}(t)$ by:

$$\theta_g = \gamma \cdot \vec{r} \cdot \int_t^{t+\Delta t} \vec{G}(\tau) d\tau \quad (5)$$

where θ_i is linked to the field inhomogeneities by:

$$\theta_i = \gamma \cdot \Delta B(\vec{r}) \cdot \Delta t \quad (6)$$

where R_{relax} describes the relaxation effects by:

$$R_{relax} = \begin{pmatrix} e^{-\frac{\Delta t}{T_2(\vec{r})}} & 0 & 0 \\ 0 & e^{-\frac{\Delta t}{T_2(\vec{r})}} & 0 \\ 0 & 0 & 1 - e^{-\frac{\Delta t}{T_1(\vec{r})}} \end{pmatrix} \quad (7)$$

and where R_{RF} represents the rotating effect of an RF pulse of phase angle ϕ leading to a flip angle α in a time τ . When no gradient are applied during the pulse R_{RF} is given (Eq. 10) by a combination of rotating matrixes about z and x axis [12]:

$$R_{RF} = Rot_z(\phi) \cdot Rot_x(\alpha) \cdot Rot_z(-\phi) \quad (8)$$

When the local experienced field is different from B_0 , an effective flip angle α' is obtained locally at each position and the R_{RF} operator takes the general form given by Eq. 11.

$$R_{RF} = Rot_z(\phi) \cdot Rot_y(\beta) \cdot Rot_x(\alpha') \cdot Rot_y(-\beta) \cdot Rot_z(-\phi) \quad (9)$$

where the effective flip angle α' is given by:

$$\alpha' = -\tau \cdot \sqrt{(\Delta\omega)^2 + \left(\frac{\alpha}{\tau}\right)^2} \quad (10)$$

and

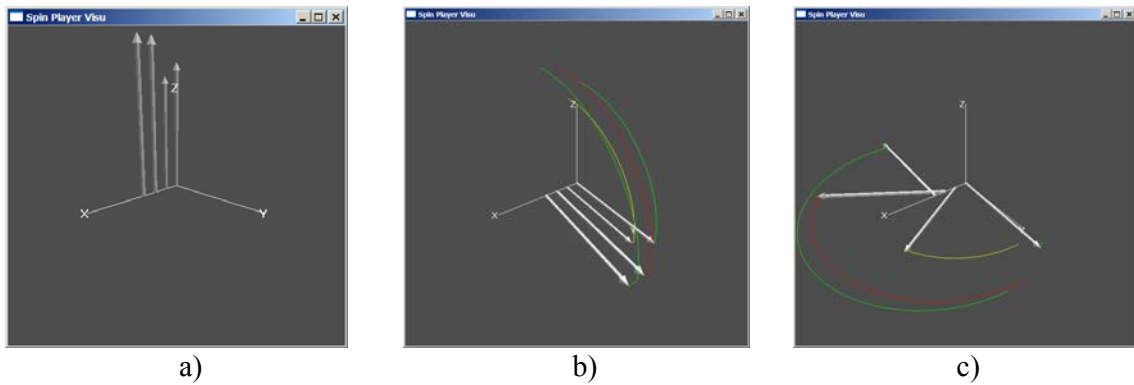
$$\beta = \tan^{-1}\left(\frac{\Delta\omega}{\alpha/\tau}\right) \quad (11)$$

where $\Delta\omega$ is local value of the frequency offset $\Delta\omega(\vec{r}, t)$ which is linked to the local field value (Eq. 2) by:

$$\Delta\omega(\vec{r}, t) = 2\pi \cdot \gamma (B_0 - B(\vec{r}, t)) \quad (12)$$

2.3 Illustrations

From Eq. [3], one can easily implement three different functions that correspond to application of RF pulse, application of gradient, and delay (i.e. spin magnetization relaxation). Figure 1 shows the evolution of four magnetization vectors during a spin echo sequence. Such kind of 1D simulation has mainly interest for pedagogic purposes.



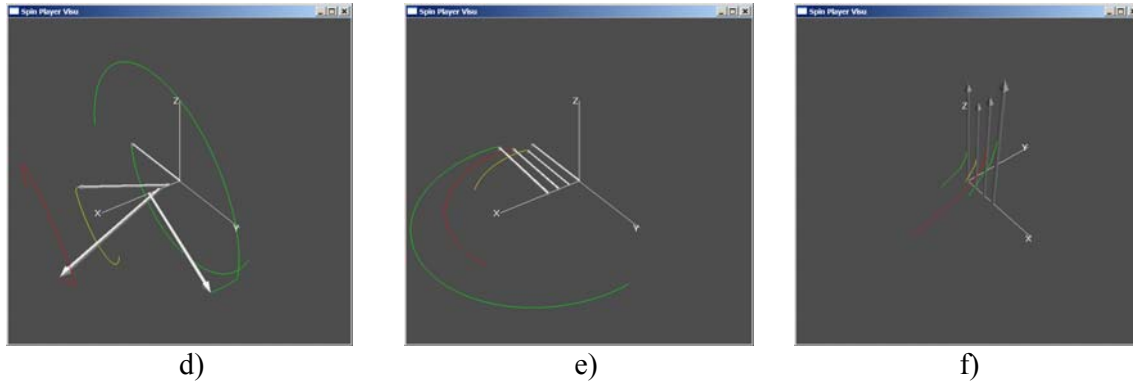


Figure 1: Illustration of 1D implementation of discrete time solution of Bloch equations. It illustrates the evolution of 4 magnetization vectors during a Spin Echo sequence. a) Equilibrium position. b) Position after a 90° RF pulse. c) Dephasing observed after application of a gradient along x direction (note that the dephasing due to T_2^* is not represented). d) Position after a 180° RF pulse. e) Rephasing after a gradient equal to the one applied in c). f) Position after a relaxation time.

3. THE SIMRI SIMULATOR

To illustrate the capability of MRI simulation based on Bloch equations, we give an overview of the *SIMRI* simulator [1] and present some results of 2D simulation like brain images obtained from the McGill Brain phantom [10] and images impacted by susceptibility artifact.

The *SIMRI* simulator is a recent 3D MRI simulator that proposes an efficient management of the T_2^* effect and integrates in a unique simulator most of the simulation features that are offered in different simulators. It takes into account the main static field value and enables realistic simulations of the chemical shift artifact including off-resonance phenomena. It also simulates the artifacts linked to the static field inhomogeneity like those induced by susceptibility variation within an object. It is implemented in the C language and the MRI sequence programming is done using high level C functions with a simple programming interface. To manage large simulations, the magnetization kernel is implemented in a parallelized way that enables simulation on PC grid architecture. Furthermore, this simulator includes a 1D interactive interface for pedagogic purpose illustrating the magnetization vector motion (as illustrated Figure 1) as well as the MRI contrasts.

3.1 Simulator overview

The simulator overview is given in Figure 2. From a 3D virtual object, the static field definition and an MRI sequence, the magnetization kernel computes a set of RF signals, i.e the k-space.

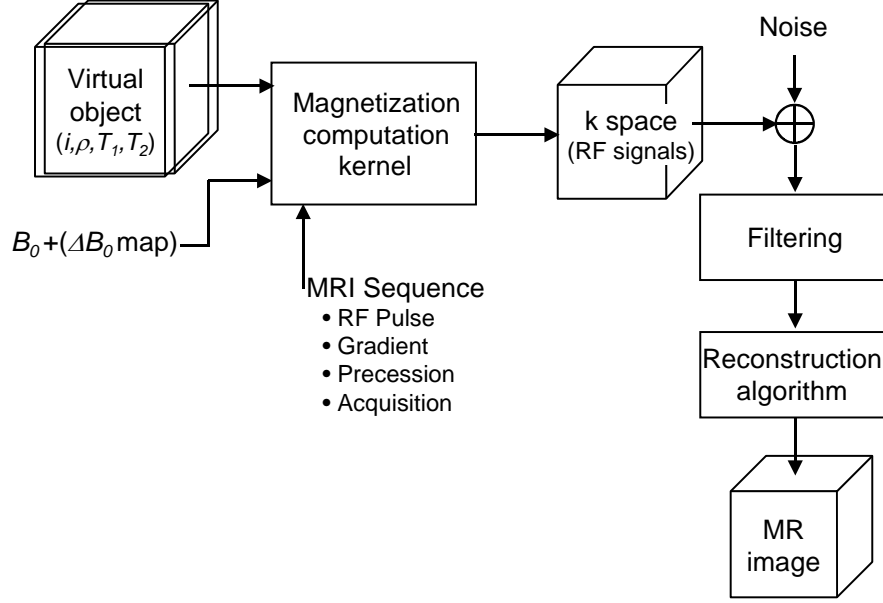


Figure 2: SIMRI Simulator overview.

The 3D virtual object is a discrete description of a real object spin system [12]. Each voxel of the virtual object contains a set of physical values that are necessary to compute the local spin magnetization vector with the Bloch equation. These values are the proton density (noted ρ), the two relaxation constants (T_1 and T_2). Moreover the type of proton must also be defined as the simulator takes into account the precession frequencies which are different for fat and water protons. A local main field inhomogeneity ΔB is also associated with each virtual object voxel (Eq. 13). ΔB corresponds to the sum of the field variation due to tissue susceptibility (ΔB_s) and other sources such as permanent field inhomogeneities (ΔB_0). It is assumed to be constant within a voxel.

$$\Delta B(\vec{r})\vec{z} = \Delta B_s(\vec{r})\vec{z} + \Delta B_0(\vec{r})\vec{z} \quad (13)$$

where $\vec{r} = (x, y, z)^T$ is the spatial coordinate.

The intra-voxel magnetic field inhomogeneity is modeled by ΔB_i which is linked to the T_2^*

by the relation $\frac{1}{T_2^*} = \frac{1}{T_2} + \gamma\Delta B_i$. This leads to a weighting of the magnetization vector amplitude by $e^{-\gamma\Delta B_i t}$ which is known as the T_2^* effect.

Four types of events can be chained to build MRI sequences: The free precession, the RF pulse, the application of gradients and the acquisition of the signal. These events are taken into account by the magnetization kernel that implements the discrete time solution of the Bloch equations detailed in section 2.2.

The RF signal acquisition corresponds to the signal reception by two orthogonal coils placed in the x,y plane of the magnetization state of the object after a given excitation. The RF signal is a one dimensional discrete complex signal that will fill in respect with the excitation sequence one line of the k-space volume. One point $s[t]$ of the RF signal is obtained by summation of the local magnetization over the entire virtual object (Eq. [14]).

The next point is obtained after an evolution of the local magnetization respecting Eq. [3] with a time step Δt equal to the sampling period of the signal.

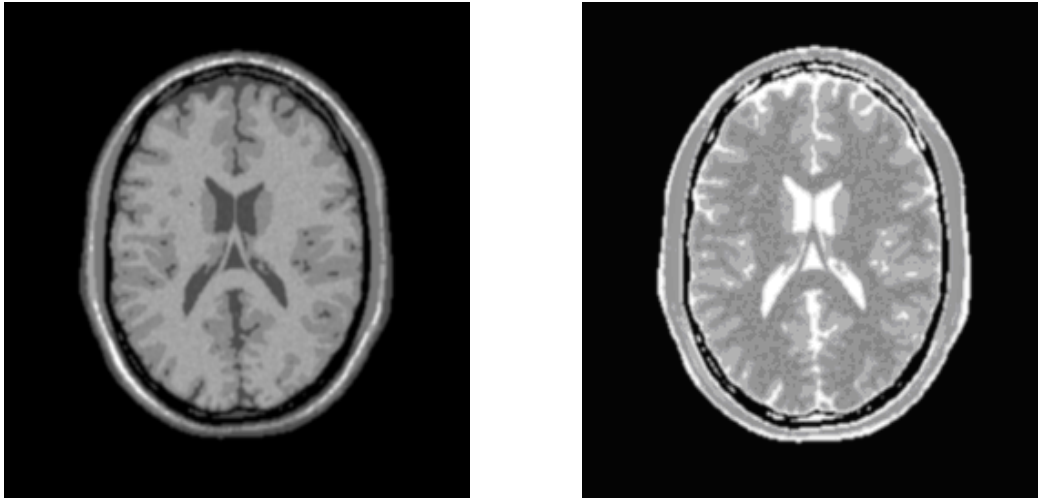
$$s[t] = \sum_{\vec{r}} \vec{M}(\vec{r}, t) \cdot \vec{x} + j \sum_{\vec{r}} \vec{M}(\vec{r}, t) \cdot \vec{y} \quad (14)$$

To simulate realistic images, noise can be added to the k-space, which can be filtered like in a real imager before the reconstruction of the MR image (Modulus and phase) using fast Fourier transform (FFT) [12].

3.2 2D simulations examples

Figure 3 and Figure 4-a present simulated brain MRI images obtained with a main field set to 1.5 T and with a virtual object based on the brain phantom of the McGill brain imaging center [13]. Only the label volume defining nine different tissues has been used with a variance of the ρ , T_1 , T_2 parameters for each tissue [10].

Figure 3-a, obtained with a 2D spin echo sequence, presents a T_1 contrast while Figure 3-b, obtained with a 2D gradient echo sequence, presents a T_2 contrast.



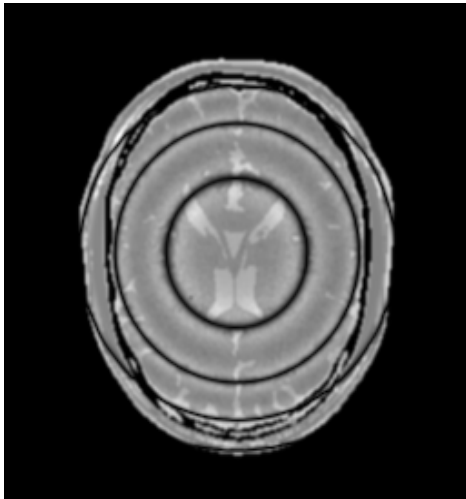
a) $TE=25\text{ ms}$ $TR=500\text{ ms}$ $BW=25.6\text{ kHz}$.

b) $\alpha = 2^\circ$ $TE=4.25\text{ ms}$ $TR=25\text{ ms}$ $BW=256\text{ kHz}$.

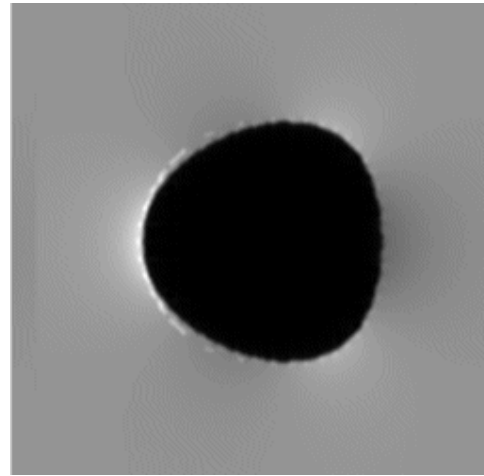
Figure 3: Contrast variation at 1.5 T on a 256x256 brain image. a) T_1 weighting using a Spin Echo sequence b) T_2 weighting using a Gradient Echo sequence.

Figure 4-a illustrates the simulation results that can be obtained when using a true-FISP sequence [14] in presence of field inhomogeneities. Indeed this sequence is very sensitive to static field inhomogeneities [15, 16] as underlined by Figure 4-a. Such artifacts are linked to the default intensity, the RF pulse angle and the TR.

Figure 4-b concerns the field inhomogeneity induced by susceptibility variation within the object. In this example, we use a 256^3 virtual object which is a spherical air bubble (diameter: 2.5 cm) within water. The precomputed field inhomogeneities [17] are taken into account by *SIMRI*. They introduce in the image geometrical and intensity distortions along the readout gradient direction as well as signal loss depending on the sequence used, the main field value, the receiver bandwidth or the echo time [18]. With a spin-echo sequence, only geometric and intensity distortions appear on the image (Figure 4-b).



a) Parabolic static field default.

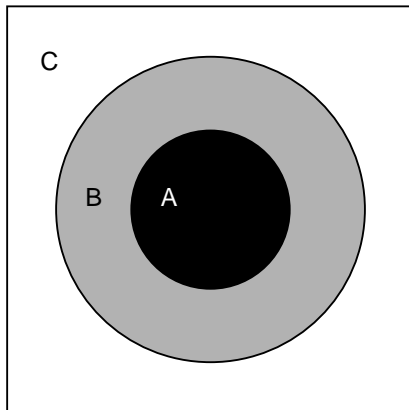


b) Susceptibility effect

Figure 4: a) True FISP simulation with an RF pulse of 20° and $300 \mu\text{s}$ duration, a readout bandwidth $BW=256 \text{ kHz}$, $TR=4 \text{ ms}$, $B_0=1.5 \text{ T}$ and a parabolic static field default with a maximum intensity of 6.10^{-5} T . b) Illustration of the susceptibility artifact on an air bubble into water with a static field of 7T . Spin Echo sequence ($TE=20 \text{ ms}$, $TR=1000 \text{ ms}$, $BW=20 \text{ kHz}$).

Figure 5 illustrates the possibilities of chemical artifact simulation thanks to the possible description of an object by many components. Here, we use two components corresponding to the water proton and the fat proton and the virtual object defined as mentioned Figure 5-a.

By simulation, it is easy to observe the impact of different parameters on the chemical shift like the readout bandwidth, the static field, or the image size. Figure 5-b presents a shift example at 7T .



a)



b) $BW=25,6 \text{ kHz}$ $N=256$

Figure 5: a) Virtual object of size 20 cm by 20 cm defined by 256×256 voxels and three regions. Region A is composed of 80% of fat protons ($T1=200$, $T2=750$) and 20% of water protons ($T1=3000$, $T2=200$). Region B is 100% water protons and region C contains no proton like air. b) Chemical shift using a Spin Echo sequence with $TE=20 \text{ ms}$ $TR=2500 \text{ ms}$ at $B_0=7 \text{ T}$ and the virtual object defined in a).

4. CONCLUSION

For twenty years, Bloch equations play a great role in the MRI simulation. Nowadays MRI simulators are able to simulate realistic MRI images including artifacts (susceptibility, chemical shift, ...). However, the amount of spin needed to properly simulate the intra-voxel dephasing due to local permanent field inhomogeneity or to simulate the dephasing induced by spoilers gradients is huge. MRI simulators must cope with this problem and propose other solutions to reduce the computation time. Many tasks are still under development like the efficient design of anatomical objects, a better modeling of the intra-voxel inhomogeneities, the introduction in the simulation process of antennas properties. Simulation of the diffusion phenomena should be achieved by using the Bloch-Torrey equations [19] with an adequate effort on the object model.

Nevertheless, the simulation of dynamic MRI imaging still appears a complex problem as it will require dynamic modeling of the object and probably another strategy of magnetization computation to avoid huge simulation time.

Finally it has to be noted that MRI simulation plays a new role by entering within image processing algorithm like the correction of MRI artifact [20].

5. REFERENCES

- [1] H. Benoit-Cattin, G. Collewet, B. Belaroussi, H. Saint-Jalmes, and C. Odet, "The SIMRI project: A versatile and interactive MRI simulator", *Journal of Magnetic Resonance*, vol. 173, pp. 97-115, 2005.
- [2] P. Shkarin and R. G. S. Spencer, "Direct simulation of spin echoes by summation of isochromats", *Concepts in Magnetic Resonance*, vol. 8, n° 4, pp. 253-268, 1996.
- [3] G. Torheim, P. A. Rinck, R. A. Jones, and J. Kvaerness, "A simulator for teaching MR image contrast behavior", *MAGMA*, vol. 2, pp. 515-522, 1994.
- [4] D. Rundle, S. Kishore, S. Seshadri, and F. Wehrli, "Magnetic resonance imaging simulator: A teaching tool for radiology", *Journal of Digital Imaging*, vol. 3, pp. 226-229, 1990.
- [5] A. R. Brenner, J. Kürsch, and T. G. Noll, "Distributed large-scale simulation of magnetic resonance imaging", *Magnetic Resonance Materials in Biology, Physics, and Medicine*, vol. 5, pp. 129-138, 1997.
- [6] M. B. E. Olsson, R. Wirestam, and B. R. R. Persson, "A Computer-Simulation Program For Mr-Imaging - Application to Rf and Static Magnetic-Field Imperfections", *Magnetic Resonance in Medicine*, vol. 34, n° 4, pp. 612-617, 1995.
- [7] D. A. Yoder, E. Changchien, C. B. Paschal, and J. M. Fitzpatrick, "MRI simulator with static field inhomogeneity", *In Proc. of SPIE Medical Imaging*, vol. 4684, pp. 592-603, 2002.
- [8] R. K.-S. Kwan, A. C. Evans, and G. B. Pike, "An extensible MRI simulator for post-processing evaluation", *In Proc. of International Conference on Visualization in Biomedical Computing, VBC'96*, pp. 135-140, 1996.
- [9] J. Bittoun, J. Taquin, and M. Sauzade, "A computer algorithm for the simulation of any nuclear magnetic resonance (NMR) imaging method", *Magnetic Resonance Imaging*, vol. 3, pp. 363-376, 1984.
- [10] R. K. S. Kwan, A. C. Evans, and G. B. Pike, "MRI simulation-based evaluation of image-processing and classification methods", *IEEE Trans. Medical Imaging*, vol. 18, n° 11, pp. 1085-1097, 1999.
- [11] F. Bloch, "Nuclear induction", *Physical review*, vol. 70, pp. 460-474, 1946.
- [12] Z. P. Liang and P. C. Lauterbur, *Principles of magnetic resonance imaging. A signal Processing perspective* New York: IEEE Press, 2000.

- [13] D. L. Collins, A. P. Zijdenbos, V. Kollokian, J. G. Sled, N. J. Kabani, C. J. Holmes, and A. C. Evans, "Design and construction of a realistic digital brain phantom", *IEEE Trans. on Medical Imaging*, vol. 17, n° 3, pp. 463-468, 1998.
- [14] A. Oppelt, R. Graumann, H. Barfuß, H. Fischer, W. Hartl, and W. Schajor, "FISP: A new fast MRI sequence", *Electromedica*, vol. 54, pp. 15-18, 1986.
- [15] L. Darrasse, L. Mao, and H. Saint-Jalmes, "Steady-state management in fast low-angle imaging", *In Proc. of SMRM Annual Meeting*, Montreal, pp. 944-945, 1986.
- [16] L. Darrasse, L. Mao, and H. Saint-Jalmes, "Fast field mapping by NMR interferometry", *In Proc. of Topical Conference on Fast MRI Techniques*, Cleveland, 1987.
- [17] S. Balac, H. Benoit-Cattin, T. Lamotte, and C. Odet, "Analytic solution to boundary integral computation of susceptibility induced magnetic field inhomogeneities", *Mathematical and Computer Modelling*, vol. 39, n° 4-5, pp. 437-455, 2004.
- [18] A. M. Abduljalil and P. M. Robitaille, "Macroscopic susceptibility in ultra high field MRI", *Journal of Computered Assisted Tomography*, vol. 23, n° 6, pp. 832-841, 1999.
- [19] H. C. Torrey, "Bloch equations with diffusion terms", *Physical review*, vol. 104, pp. 563-565, 1956.
- [20] B. Belaroussi, Y. Zaim-Wadghiri, H. Benoit-Cattin, C. Odet, and D. H. Turnbull, "Distortion correction for susceptibility-induced artifacts in spin echo MR images: Simulation study at 1.5 T and 7 T.", *In Proc. of ISMRM'04*, Tokyo, pp. 2168, 2004.